Evidence of strong flux pinning in melt-processed ternary (Nd–Eu–Gd)Ba 2 Cu 3 O y superconductors

A. K. Pradhan, M. Muralidhar, M. R. Koblischka, M. Murakami, K. Nakao, and N. Koshizuka

Citation: Applied Physics Letters **75**, 253 (1999); doi: 10.1063/1.124339
View online: http://dx.doi.org/10.1063/1.124339
View Table of Contents: http://scitation.aip.org/content/aip/journal/apl/75/2?ver=pdfcov
Published by the AIP Publishing

Evidence of strong flux pinning in melt-processed ternary (Nd–Eu–Gd)$Ba_2Cu_3O_y$ superconductors

A. K. Pradhan,[a] M. Muralidhar, M. R. Koblischka, M. Murakami, K. Nakao, and N. Koshizuka
Superconductivity Research Laboratory, ISTEC, 1-10-13, Shinonome, Koto-ku, Tokyo 135-0062, Japan

(Received 21 December 1998; accepted for publication 14 May 1999)

The flux pinning behavior of ternary melt-processed (Nd–Eu–Gd)$Ba_2Cu_3O_y$ superconductors is studied with varying defect concentrations using magnetotransport and magnetization measurements. A huge field-induced bump feature in the resistivity with increasing defect density, field-induced magnetization kink and linear voltage-current *(V-I)* characteristics over the whole transition temperature regime favor the phenomenon of vortex entanglement in the liquid phase. The Nd/Ba substitution sites along with the fine second-phase particles are one of the possible reasons for the vortex entanglement and these defects give rise to high critical current density and reduced dissipation at low temperature with significant enhancement in pinning. © *1999 American Institute of Physics.* [S0003-6951(99)00128-X]

Many attempts have been put forward to enhance the critical current density J_c in layered high- T_c superconductors to harness their applications at 77 K. Several ways of implementing this strategy include reducing CuO_2 layer separation, metallizing the blocking layers, chemical substitution and introducing columnar defects. The recent development[1,2] of $NdBa_2Cu_3O_y$ under controlled atmosphere and oxygen-controlled melt-growth (OCMG) processed ternary (LRE)BaCuO (where LRE=light rare-earth elements, i.e., Nd, Sm, Eu, Gd) superconductors[3–5] has opened up a new insight for power applications because of their high J_c ($\geqslant$20 000 A/cm^2) at 77 K and $T_c \geqslant 95$ K. A solid solution between the LRE atoms and Ba provides additional flux pinning due to the composition fluctuation in the sample leading to spatial variations of T_c. Further flux pinning can be provided by $(LRE)_2BaCuO_5$ (211) particles which can be added to the starting powders as is done in YBCO. This increased pinning can be explained as due to δT_c (spatial variation of T_c) or $\Delta\kappa$ pinning (variation of the order parameter).[5]

In this letter, we report the resistive transitions in magnetic fields, the voltage-current *(V-I)* characteristics and magnetization for several NEG samples with varying degrees of second-phase additions. We observe that the vortex viscosity increases remarkably with the addition of the second phase, promoting the vortex entanglement in the liquid phase. Our results strongly suggest that the viscosity of the vortex liquid state increases due to the spatial variation of T_c and with the addition of the second phase with Pt.

Bulk samples of $(Nd_{0.33}Eu_{0.33}Gd_{0.33})Ba_2Cu_3O_y$ (NEG) were prepared using the OCMG process in 0.1% O_2 partial pressure. A series of samples with additions of 10–40 mol % NEG-211 was prepared. In order to refine the resulting 211 particle size, 0.5 mol % Pt was added. The crystallization process was initialized by a MgO (100) seed. Details of the heat treatment are described elsewhere.[6] The samples chosen for this study were (i) NEG-A, a pure sample without any additions (dimension, $d=0.248\times0.214\times0.084$ cm^3), (iii) NEG-B with 10 mol % 211 ($d=0.14\times0.135\times0.098$ cm^3) and NEG-C with 20 mol % 211 ($d=0.164\times0.130\times0.054$ cm^3).

A standard ac technique (with $I=1$ mA, $f=17$ Hz) was used to measure the resistivity for the $H\|c$ axis of the sample using a low-noise ratio transformer. Isothermal *V-I* characteristics were measured using the dc method. The magnetization measurements were performed in a commercial superconducting quantum interference device (SQUID)[7] magnetometer using a 1 cm scan length in continuous temperature sweep mode with a sweep rate $dT/dt=35$ mK/min.

The resistive transitions in various fields for samples NEG-A, B, and C are shown in Fig. 1. NEG-A shows a foot with a larger transition width compared to the NEG-B and -C samples. The most distinguishing difference among these samples is that NEG-B and -C display a huge broad bump (''giant bump'' feature) at about 50% of the resistive transition for higher magnetic fields. Although a very small bump feature is observed for NEG-A in high fields, it is not observed for $H\leqslant2$ T. We have shown the relative magnitude of the bump feature of the NEG-B sample at $H=7$ T in the inset of Fig. 1. It should be noted that there is a remarkable rise of the bump feature with decreasing temperature that falls sharply once the temperature is lowered below the temperature for the peak in the bump feature, T_b. However, this feature diminishes in size for a sample containing 30% of the second phase with Pt (NED-D, not shown here). The distinguishing feature of all these curves is that the bump feature is a strong function of the field. The down turn in resistance below T_b is due to strong pinning. The large reduction in the normal state resistivity in NEG-B compared to in NEG-A ($\sim$400 $\mu\Omega$ cm at 96 K for NEG-A drops to $<$200 $\mu\Omega$ cm at 96 K for NEG-B and -C) is due to Pt addition that creates percolating paths due to the proximity effect that allows currents to flow more easily. Furthermore, Pt refines 211 particles, which contribute to the bump feature, to submicron size.[6]

In order to prove the existence of additional pinning centers originating from a weaker superconducting phase, we show the temperature dependent magnetization for NEG-B in Fig. 2 for various fields in field cooling (FCC) that was

[a]Electronic mail: pradhan@istec.or.jp

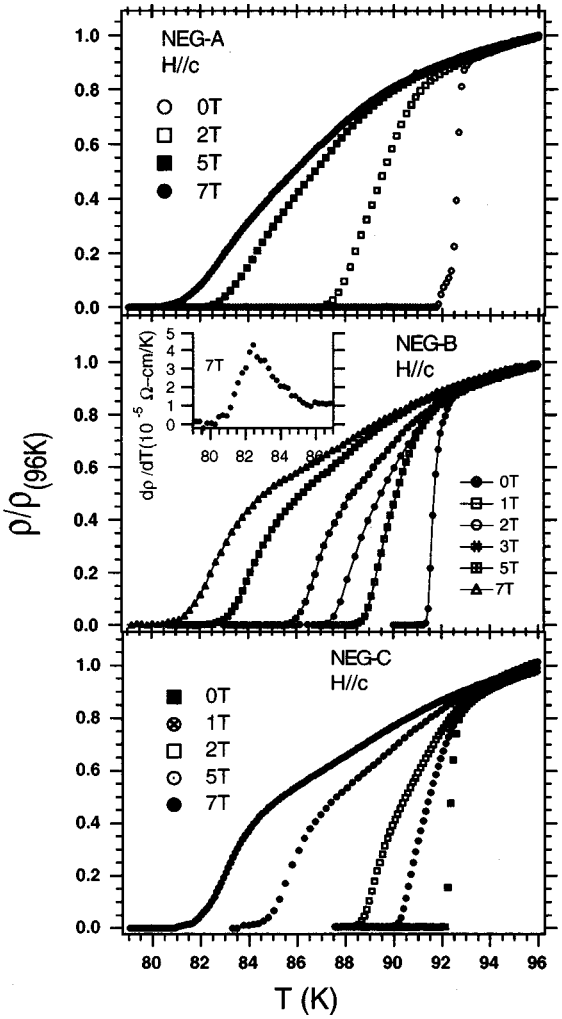

FIG. 1. Temperature dependence of the resistivity of NEG-A, NEG-B, and NEG-C samples at various magnetic fields, $H\|c$ axis. The inset shows $d\rho/dT$ in NEG-B near the transition regime.

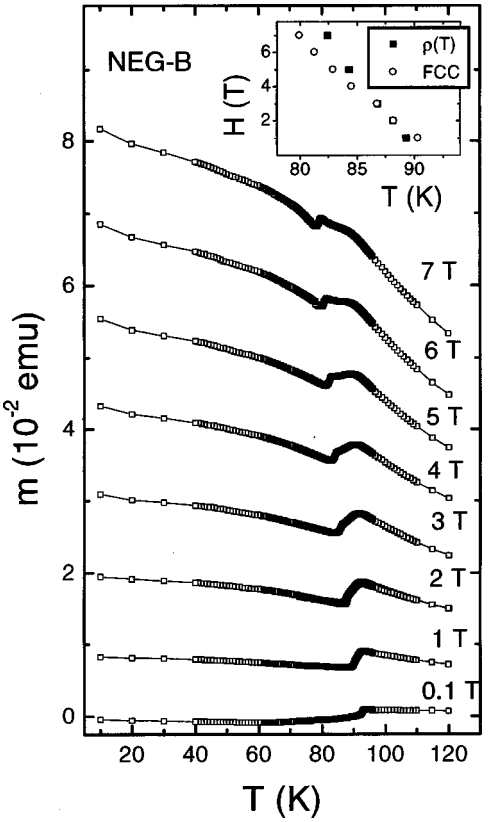

FIG. 2. Temperature dependence of the magnetization of the NEG-B sample at various magnetic fields for the $H\|c$ axis using a FCC mode. The inset shows the field dependent T_b in the magnetoresistance and the corresponding kink in the magnetization for NEG-B.

reported earlier.[5] These curves show that the magnetic moment is always positive and increases with increasing field and decreasing temperature following Curie-Weiss law. This clearly shows the contribution from the paramagnetic moment of Nd and Gd. The most important observation is the step feature; more distinct is a kink in the magnetization that is a strong function of the magnetic field, similar to the bump feature in magnetoresistance. Note that the temperatures corresponding to the kink in the magnetization and the bump in the resistivity are very close to one another as is shown in the inset of Fig. 2 for NEG-B. This is a clear indication of a transition in the vortex state and most probably it is caused by δT_c due to LRE substitution at the Ba site.

In Fig. 3, we show the field dependent J_c for three samples at 77 K. There is a remarkable increase in J_c with the addition of the second phase and Pt. However, an excess addition of the second phase decreases the irreversibility field, $H_{\rm irr}$ (in NEG-D) although the J_c value remains much higher than that for the NEG-A sample. Using an approach for pinning force discussed earlier,[8] we show the normalized pinning force, $F_p/F_{p,\max}$ as a function of reduced field in the inset of Fig. 3. The peak position $h=H_a/H_{\rm irr}\sim 0.5$ corresponds to δT_c or $\Delta\kappa$ pinning as observed microscopically.[9]

It is very important to understand the behavior of the vortex state in the presence of the above mentioned defects. The fast drop of the resistance below T_b is a consequence of pinning in the liquid state which indicates that the vortex liquid is highly viscous, a possible signature of *vortex entanglement*.[10] The increased relative importance of such disorders at high fields comes from the instability of the vortex structure against lateral vortex displacements[11] which become larger at high fields. Thus, by adding more smaller

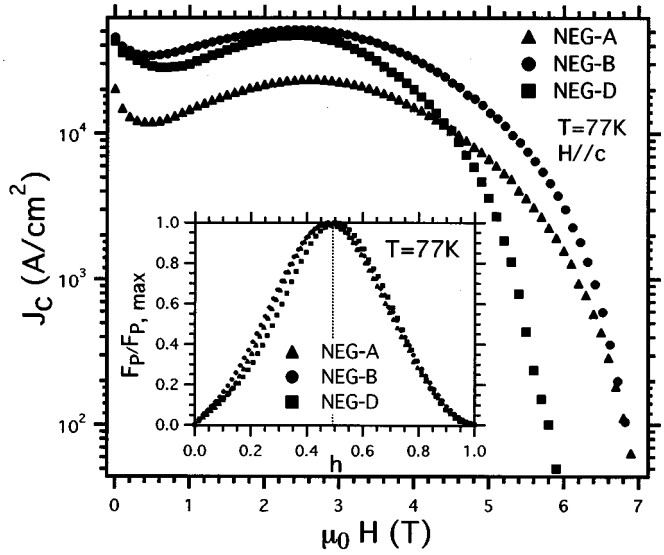

FIG. 3. Field dependence of the critical current density, J_c at 77 K for NEG-A, NEG-B, and NEG-D containing 30 mol % second-phase and 0.05% Pt. The inset shows the normalized pinning force density as a function of reduced field, $h=H_a/H_{\rm irr}$.

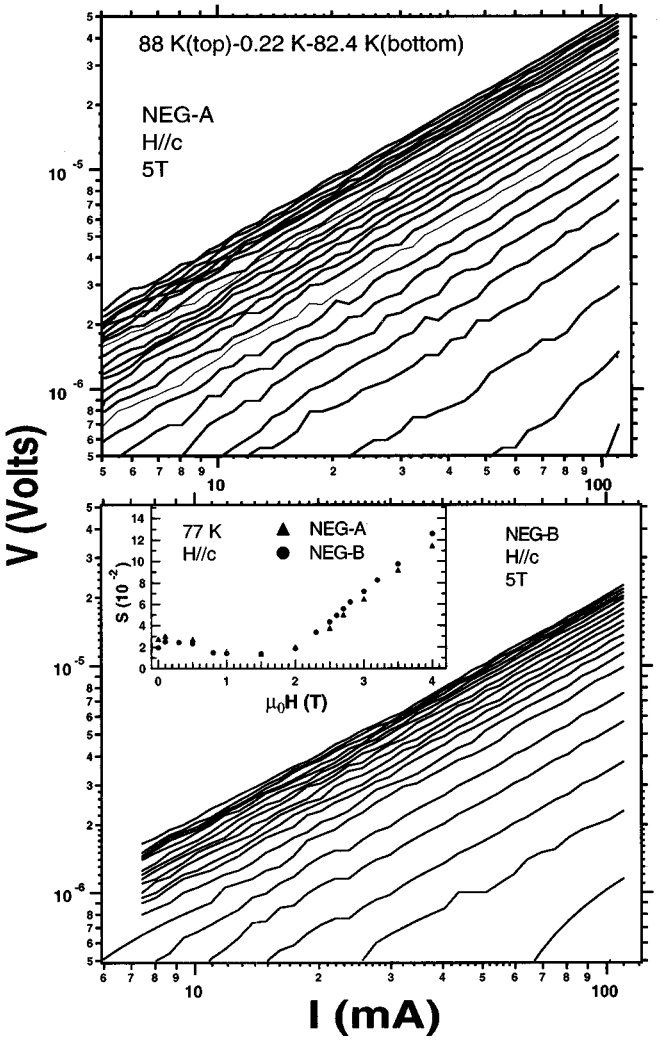

FIG. 4. Voltage-current characteristics of NEG-A for a small temperature interval of 0.22 K and NEG-B in a temperature interval of 87 K (top) and −0.2, −84.2, −0.5, −81.7 K (bottom) for the $H=5$ T applied $\|c$ axis.

defects, the defect density increases in the liquid state rendering the liquid state more viscous with increased pinning. The enhanced bump feature in NEG-B and -C is the direct consequence of this phenomenon. However, we believe that vortex entanglement takes place in all the samples studied here. In order to test this, we present *V-I* characteristics of NEG-A and NEG-B in a field of 5 T for the $H\|c$ axis. All *V-I* curves yield linear behavior throughout the entire transition region. Similar *V-I* curves were reported[12] in an electron irradiated YBCO single crystal in which sufficient point defects were produced. It may be noted that such defects act as pinning centers due to δT_c pinning. This dynamic response is consistent with that of an entangled liquid that will require nucleating in-plane vortex loops. One intriguing recent approach generates relevant loops[13] via vacancies and interstitials proliferating in the vortex lattice at high fields. Nd/Ba substitution sites and 211 second-phase particles dislocation glide perpendicular to the basal plane are reported[14] to be present in Nd123 material. The most important characteristic of vortex entanglement is that it grows with the increasing field and with the increase of defect density as well. The linear rise of T_b with field shown in the inset of Fig. 2 confirms this. Since the field-induced pinning centers (of the order of a few nm to a few tens of nm)[9] are the major contributor to pinning in NEG samples, the formation of such an entangled state is one possible reason.

The strong pinning arises when this entangled state freezes into a glassy phase. Experimentally, the tail of our resistive transition can be fit to a power law $\rho\sim(T-T_c)^{\alpha}$, only with a field dependent exponent $\alpha(H)$ varying from 1.5 to 4.5 with increasing field, reflecting increased pinning in the liquid phase. Hence the dissipation becomes negligible far from the putative glass transition. The normalized magnetic relaxation rate, S ($S=-M_0^{-1}(dM/d\ \ln\ t)$, M_0 is the initial magnetic moment at time, $t_b\sim 60$ s) shown in the inset of Fig. 4 predicts that the dissipation is very small indeed at 77 K. Another remarkable feature in the magnetic relaxation is the observation of a plateau in the intermediate field range which is possibly due to the collective pinning nature[15,16] of the pinning centers.

In conclusion, we have demonstrated evidence of a strong pinning behavior in the dynamics of vortex liquid that renders a very high J_c at 77 K in NEG samples. By means of magnetotransport and magnetization measurements, we have shown that the dense viscous nature of the liquid phase arises from the pinning centers such as Nd/Ba substitution sites leading to the spatial variation of T_c favoring vortex entanglement that grows with increasing field and defect density in the liquid state. The addition of the second phase and its subsequent refinement by Pt addition enhance the pinning strength significantly. These studies provide insight into the understanding of the vortex pinning nature in ternary NEG samples for their potential as power applications.

This work was partially supported by the New Energy and Industrial Technology Development Organization (NEDO). Two of the authors (M.R.K. and M.M.) were supported by STA and by the Iwate Techno Foundation.

[1] S. I. Yoo, N. Sakai, H. Takaichi, T. Higuchi, and M. Murakami, Appl. Phys. Lett. **65**, 633 (1994).
[2] T. Egi, J. G. Wen, K. Kuroda, H. Unoki, and N. Koshizuka, Appl. Phys. Lett. **67**, 2406 (1995).
[3] M. Murakami, N. Sakai, H. Takaichi, T. Higuchi, and S. I. Yoo, Supercond. Sci. Technol. **9**, 1015 (1996).
[4] M. Muralidhar, H. S. Chauhan, T. Saito, K. Kamada, K. Segawa, and M. Murakami, Supercond. Sci. Technol. **10**, 663 (1997).
[5] M. R. Koblischka, M. Muralidhar, and M. Murakami, Appl. Phys. Lett. **73**, 2351 (1998).
[6] M. Muralidhar, M. R. Koblischka, and M. Murakami, Supercond. Sci. Technol. **11**, 1349 (1998).
[7] Quantum Design, San Diego, CA, **291**, model XL.
[8] A. K. Pradhan, K. Kuroda, B. Chen, and N. Koshizuka, Phys. Rev. B **58**, 9498 (1998), and references therein.
[9] W. Ting, T. Egi, K. Kuroda, N. Koshizuka, and S. Tanaka, Appl. Phys. Lett. **70**, 770 (1997).
[10] D. R. Nelson, Phys. Rev. Lett. **60**, 1973 (1988).
[11] G. Blatter, M. V. Feigel'man, V. B. Geshkenbein, A. I. Larkin, and V. M. Vinokur, Rev. Mod. Phys. **66**, 1125 (1994).
[12] J. A. Fendrich, W. K. Kwok, J. Giapintzakis, C. J. van der Beek, V. M. Vinokur, S. Fleshler, U. Welp, H. K. Viswanathan, and G. W. Crabtree, Phys. Rev. Lett. **74**, 1210 (1995).
[13] E. Frey, D. R. Nelson, V. M. Vinokur, and D. S. Fisher, Phys. Rev. B **49**, 9723 (1994).
[14] F. Sandiumenge, N. Vilalta, J. Rabier, and X. Obradors, Appl. Phys. Lett. **73**, 2660 (1998).
[15] P. J. Kung, M. P. Maley, M. E. McHenry, J. O. Willis, M. Murakami, and S. Tanaka, Phys. Rev. B **48**, 13922 (1993).
[16] A. K. Pradhan, B. Chen, W. Ting, K. Kuroda, K. Nakao, and N. Koshizuka, Supercond. Sci. Technol. **11**, 408 (1998), and references therein.